Citation: Proceedings of SPIE Vol. 8777 87771D (2013)
https://doi.org/10.1117/12.2017444

Multilayer reflective polarizers for the far ultraviolet

Juan I. Larruquert[1*], José A. Aznárez[1], Luis Rodríguez-de Marcos[1], José A. Méndez[1], A. Marco Malvezzi[2], Angelo Giglia[3], Paolo Miotti[4], Fabio Frassetto[4], Giuseppe Massone[5], Stefano Nannarone[6], Giuseppe Crescenzio[5], Gerardo Capobianco[5], Silvano Fineschi[5]

[1]GOLD, Instituto de Óptica-Consejo Superior de Investigaciones Científicas, Madrid, Spain
[2]Universitá di Pavia, Pavia, Italy
[3]Istituto Officina dei Materiali -Consiglio Nazionale delle Ricerche, Trieste, Italy
[4]Institute of Photonics and Nanotechnologies-National Council for Research, Padua, Italy
[5]INAF - Osservatorio Astrofisico di Torino, Torino, Italy
[6]Dipartimento di Ingegneria dei Materiali e dell Ambiente, Universita di Modena e Reggio Emilia, Modena, Italy

ABSTRACT

Polarimetry in the far ultraviolet (FUV) is a powerful tool for the interpretation of the role of the coronal plasma in the energy transfer processes from the inner parts of the Sun to the outer space. FUV polarimetry from space provides more accurate observations on the kinetics of the features and on local magnetic fields through the Doppler and Hanle resonant electron scattering effects. Particularly interesting lines for FUV polarimetry are H Lyman α (121.6 nm) and β (102.6 nm), along with OVI lines at 103.2 and 103.8 nm. One key element to perform polarimetry measurements at these wavelengths is the need of efficient polarizers. A limitation of the available polarizers, such as crystal plates of MgF_2 and LiF working at Brewster angle, is their moderate reflectance at the non-extinguished component of the electric field, which results in a modest polarizer efficiency.

Research is underway to develop efficient polarizers operating in the short FUV based on reflective multilayer coatings. First wavelength target is 121.6 nm. We have obtained promising preliminary results with $(Al/MgF_2)_3$ multilayer polarizers. Their reflectance for both s (TE) and p (TM) polarization has been measured as a function of the angle of incidence and wavelength at BEAR beamline of ELETTRA synchrotron. The analysis of the first campaign enabled refining the designs for a second campaign, which has resulted in efficient polarizers in a range around 121.6 nm. Future research will address the stability of these polarizers both in atmosphere and in relevant conditions for space optics.

Keywords: polarizers, multilayer coatings, far ultraviolet, vacuum ultraviolet, polarimetry, solar corona, Hanle effect

1. INTRODUCTION

Measuring magnetic fields in the solar corona is crucial to understanding and predicting the Sun's generation of space weather that affects communications, space flight, and power transmission. Most outputs of solar activity, including high-energy electromagnetic radiation, solar energetic particles, flares and coronal mass ejections, derive their energy from the coronal magnetic field. The corona is also the source of the solar wind, having its own embedded magnetic field that engulfs the Earth's magnetosphere. Because the changing coronal magnetic field drives the processes at the origin of space weather, the ability to measure the field changes will enable us to understand the basic underlying physics and predict space weather events. The measurement of the solar magnetic field requires polarimetric observations in appropriate spectral lines. Signals with partially linear polarization are expected for many of the permitted ultraviolet (UV) and far-UV (FUV; it will refer here to wavelengths shorter than 200 nm) line-emissions from the solar corona. The line-emission linear polarization is caused by anisotropic radiation pumping processes, which induce atomic polarization in the energy levels involved in the transition of the emitted radiation. The magnetic field modifies this linear polarization through the Hanle effect, thus leaving information on its strength and

* larruquert@io.cfmac.csic.es; phone: 34- 915618806 ext 330; fax: 34-914117651

orientation in the emergent Stokes parameters, regardless of how large the line width due to Doppler broadening is.

Among the brightest lines sensitive to the Hanle effect is the H I Lyman-α line at 121.6 nm[1,2,3,4,5,6]. The Hanle effect in the H I Lyman-α line is sensitive to both the field direction and magnitude between 10 and 250 G, centred on the so-called typical (or critical) field that is 53 G for this line[7]. It was shown[2, 8] that a degree of polarization of up to 20% can be expected in the H I Lyman-α line in the solar corona. Using the SOHO/SUMER spectrograph, Raouafi et al.[9, 10] achieved the first detection of the Hanle polarization signal in the corona using the O VI doublet at 103.2/103.8 nm. These pioneering results were obtained with an instrument that was not designed to measure polarization and they established without any ambiguity that a dedicated instrument will be able to provide routine global coronal magnetic field diagnostics.

H I Lyman-β (102.6 nm) and Lyman-γ (97.3 nm) lines are sensitive to weaker magnetic fields than the H I Lyman-α line, with typical fields being 16 and 7 G respectively[7,3,4]. Such weaker fields are expected to exist outside of active regions. However, the H I Lyman-α line is by far the strongest line in the FUV/UV range of the solar spectrum and will provide us with sufficient signal-to-noise ratio. Therefore, observations of the Hanle effect in the H I Lyman-α line are the ideal tool for the coronal magnetic field diagnostics in active regions.

Linear polarizers is one of the basic elements for polarimetry; the other is phase retarders. Linear polarizers, which will be plainly called polarizers in the following, are able to turn incoming radiation that was nonpolarized or elliptically polarized (or a mixture of the two) into linearly polarized in a specific direction. Efficient polarizers at Lyman α are needed for observations to examine the solar magnetic field. Moreover, polarizers operating at short wavelengths are needed for an always increasing number of applications, including imaging instrumentation for solar physics and astrophysics, ellipsometry, synchrotron radiation, lasers, particle-matter interaction, atomic and molecular physics, solid state physics, magnetic and chiral-material analysis, etc.

The simplest polarizers at 121.6 nm and at most of the FUV are crystal plates of transparent fluorides, namely MgF_2 and LiF, working in reflection at Brewster angle. One limitation of these elements is their modest reflectance at the non-extinguished component of the electric field, which results in a moderate polarizer efficiency. Thus, at 121.6 nm a MgF_2 plate at Brewster angle will not reflect the p (TM) polarized component of the incoming light, hence R_p=0, but the s component (TE), R_s, at this same angle is low for an application where radiation is not intense. Polarizers at Brewster angle can also operate by transmittance, due to the increased T_p/T_s ratio of the beam transmitted through a plate; FUV polarizers based on a pile of plates in series have been prepared[11]. FUV polarizers based on the birefringence of MgF_2 are also possible[12]. They are produced in the geometry of, for instance, Rochon prisms, which deviate the extraordinary ray and keep the ordinary ray undeviated. Rochon prisms are used in the FUV; however, the birefringence of MgF_2 is small at 121.6 nm, which makes it difficult to separate the two beams.

Efficient polarizers can be developed with the use of multilayer coatings. Not much research has been devoted yet to polarizing coatings covering the wavelength of 121.6 nm. Hass and Hunter[13] developed a 3-mirror polarizer, with the benefit of no deviation of the incoming beam; it combined two Al/MgF_2 mirrors and a MgF_2 plate working close to Brewster angle; it had a good R_s/R_p efficiency ratio in a wide spectral range including the FUV and shortwards, but it had a modest efficiency for the non-extinguished component of ~17% close to 121.6 nm. Yang et al.[14] proposed Au-SiC-Au, 3-mirror reflection polarizers, which can be operative in a wide band including the FUV and shortwards, with the additional gain of suppressing higher diffraction orders. Kim et al.[15] designed a polarizer for 121.6 nm based on a 3-layer $MgF_2/Al/MgF_2$ coating deposited on an Al substrate. Bridou et al.[16] prepared single pair polarizing coatings of AlF_3 and of MgF_2 on glass, tuned at 103.2 and 121.6 nm, respectively. Bridou et al.[17] reported on efficient polarizers at 121.6 nm based on various coatings: a single layer of MgF_2 on glass, a single pair of MgF_2/AlF_3 on glass, a single pair of SiO_2/MgF_2 on fused silica, and a $(Al/MgF_2)_2$ four layer coating on glass. Kano et al.[18] fabricated a polarizer based on the $(Al/MgF_2)_2$ polarizer design of Ref. 17, and obtained a good efficiency at 121.6 nm.

This proceeding presents the research performed on reflection polarizers optimized to operate at the wavelength of 121.6 nm and in the close spectral range. The coating is based on $(Al/MgF_2)_n$ mutilayers. Section 2 describes the experimental techniques used for coating deposition and polarizer characterization. Section 3 presents some details on the material selection and the coating design and it displays the FUV reflectance measurements on $(Al/MgF_2)_n$ polarizing coatings.

2. EXPERIMENTAL EQUIPMENT

2.1 Sample preparation

Polarizing multilayer coatings were prepared at GOLD. $(Al/MgF_2)_n$ multilayer coatings (Al is always the first layer and MgF_2 the last one) were deposited in a high vacuum chamber pumped with a turbomolecular system and a liquid-N_2 cooled, Ti sublimation pump. The base pressure was 10^{-5} Pa. Films of Al and MgF_2 were deposited by evaporation using tungsten multi-stranded filaments (Al), and W boats (MgF_2); the evaporant material was 99.999% pure Al and VUV-grade MgF_2; the deposition rate was ~1.0 (Al) and ~0.7 (MgF_2) nm/s; pressure during deposition was ~10^{-4} (Al) and ~$5x10^{-5}$ (MgF_2) Pa. Films were deposited onto non-intentionally heated or cooled polished float glass substrates. The deposition source-substrate distance was 30 cm. Film thickness was measured with a quartz-crystal monitor, previously calibrated through Tolansky interferometry, i.e., through multiple-beam interference fringes in a wedge between two highly reflective surfaces[19].

2.2 Experimental setup for reflectance measurements

The polarization characteristics of the coatings were measured at Bending magnet for Emission, Absorption and Reflectivity (BEAR) beamline of ELETTRA synchrotron (Trieste, Italy)[20,21,22]. Reflectance measurements were performed between 8 eV (155.0 nm) and 12 eV (103.3 nm); for higher order rejection we used a 0.5-mm thick LiF crystal made by Crystec. Measurements were performed with exit slits opened at 900x400 μm^2: with this configuration the spot size on the sample was 400x400 μm^2 and the bandwidth was 60 meV FWHM. The detector was a silicon diode IRD-SXUV100; the background was subtracted for each measurement.
Measurements with polarized radiation are possible due to the polarization properties of the bending magnet source, which depend on the emission angle. This radiation is linearly polarized in the storage ring plane and elliptically polarized outside. To get linearly polarized light we used the polarization selector[23], a variable aperture double slit mechanism that can be positioned vertically to deliver alternatively linear, right or left circular polarization light. Measurements have been made in linear polarization configuration, i.e. with the polarization selector centered with respect to the beam source in the vertical direction (perpendicular to the ring plane). The selector slits were set to have a vertical acceptance of 4 mm, which correspond to an angular aperture of ±0.17 mrad. With this configuration, the calculated degree of linear polarization of the beam is: $(I_s-I_p)/(I_s+I_p)=0.99$, where I_s and I_p stand for the incident beam intensity with the electric vector perpendicular and parallel, respectively, to the plane of incidence. Reflectance measurements were performed in two perpendicular planes of incidence, for which the experimental chamber was rotated 90° around the beam axis. The role of s and p are interchanged when the chamber rotates 90°.

3. RESULTS AND DISCUSSION

The materials considered in the design of the polarizing coating were Al and MgF_2. They are a natural choice because MgF_2 is among the few transparent materials at 121.6 nm and the refractive index of Al has a strong contrast to the one of MgF_2. The other possible transparent materials are LiF and AlF_3, but there is a much more limited experience on coatings combined with Al films, except for mirrors of Al protected with a thin film of LiF[24]; furthermore, LiF is less stable than MgF_2 in a humid atmosphere. There is also one piece of research on Al protected with an AlF_3 layer[16]. Another choice of material contrasting with MgF_2 would be Mg[25,26,27]; in fact the latter has become a common material in multilayers for wavelengths slightly longer than Mg $L_{2,3}$ edge (~25.1 nm) [28,29]; however, no literature has been found on multilayers combining Mg with MgF_2. In contrast, there is a long heritage on stable and efficient mirrors based on Al protected with a thin film of MgF_2[30]. There is also literature on the use of $(Al/MgF_2)_n$ multilayer coatings[31,32,33,34,35], mostly for transmittance filters peaked in the FUV. Efficient polarizers based on this combination of materials were developed by Bridou et al.[17]. The same material combination was selected here.

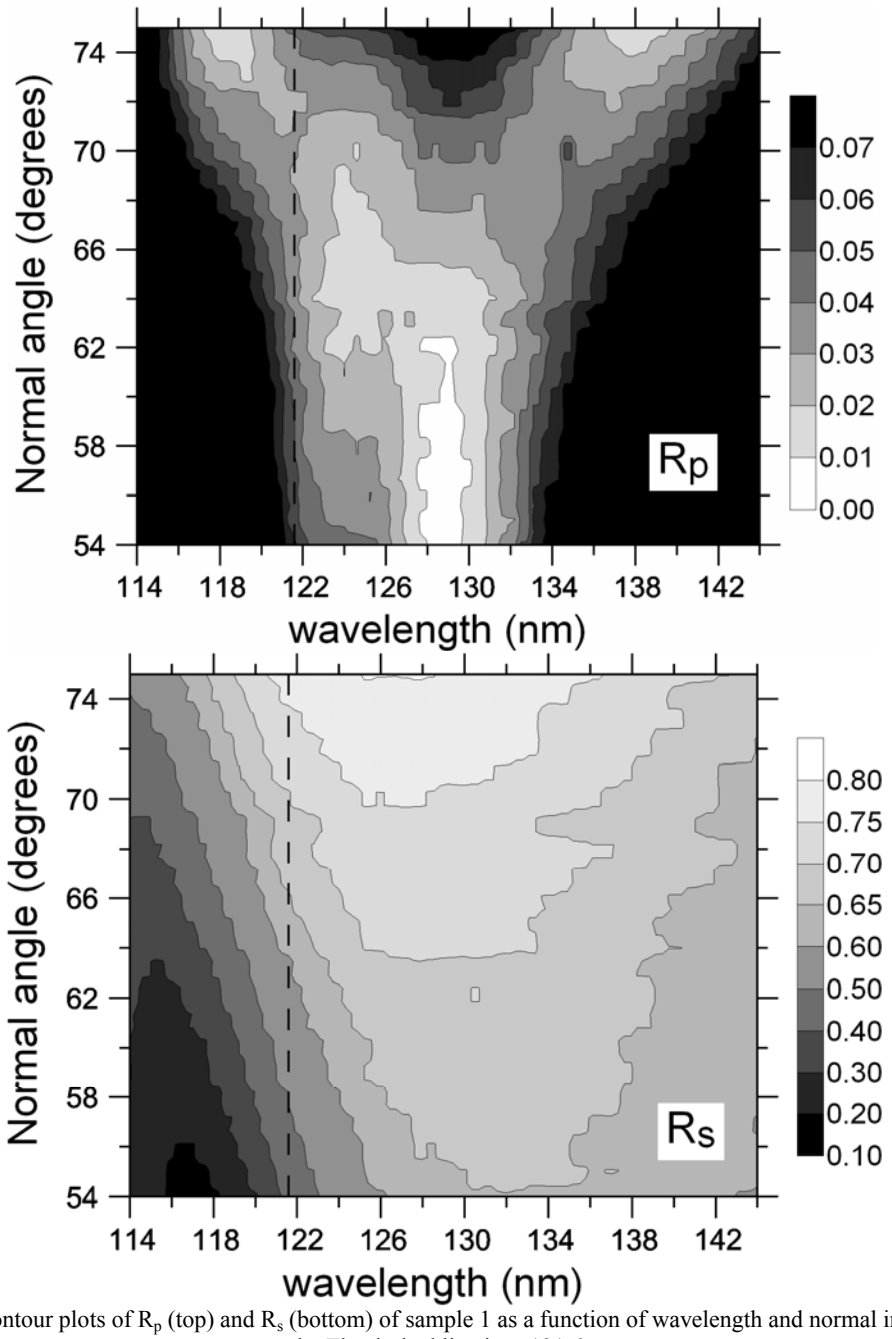

Fig. 1. Contour plots of R_p (top) and R_s (bottom) of sample 1 as a function of wavelength and normal incidence angle. The dashed line is at 121.6 nm

Designs with various numbers of Al/MgF_2 bilayers have been evaluated. The polarizing coatings will be described through their reflectance in the two planes of incidence, R_s and R_p. Increasing the number of adjustable parameters favours an increase in the spectral and angular bands with both a high R_s and R_s/R_p ratio. For this reason, designs with at least three bilayers were selected. There is a higher limit to the total Al thickness that can be accumulated through the different layers in order to enable radiation to penetrate in the multilayer; there is also a lower limit in the minimum film thickness in each layer for the film to be continuous and to be described through a uniform refractive index. These constraints result in an upper limit to the maximum number of bilayers that can be used. For the above reasons, designs with not more than four bilayers have been selected here. Summarizing, coatings with 3 and 4 Al/MgF_2 bilayers have been designed and prepared in this research. The coatings were optimized to have simultaneously the largest possible R_s and R_s/R_p ratio around 121.6 nm and around the target incidence angle. To satisfy this, it is critical to obtain values of R_p close to 0. When the incidence angle is large enough, a large R_s value can be obtained at the same wavelength and angle that the minimum R_p; all incidence angles are here referred to the normal to the coating surface. R_p and R_s for a fraction of the prepared samples has been measured so far, and measurements on $(Al/MgF_2)_3$ coatings are presented below.

This research has been conducted through two campaigns; in each campaign we designed and prepared polarizing coatings that were measured at the beamline. Fig. 1 displays the reflectance measured for an $(Al/MgF_2)_3$ sample prepared in the first campaign, which is here called sample 1; the figure displays both R_p (top) and R_s (bottom) as a function of wavelength and the incidence angle. In Fig. 1, the angle step was 1º and the spectral scanning was made in photon energy steps of 0.05 eV. The sample was measured ~2 weeks after deposition; the sample was in contact with normal air for about one week. The coating had been optimized at 121.6 nm at 60º, where it was measured R_p=0.048 and R_s=0.53. Fig. 1 shows that a lower R_p was measured at wavelengths longer than 121.6 nm. A reflectance below 0.01 was measured in the 127.5-130.0-nm range for angles in the 54°-62° range, where R_s stood in the range of 0.63 (127.5 nm at 54º) to 0.70 (130 nm at 62º).

The experience accumulated in the first campaign helped in refining the designs for the second campaign. A sample similar to the one presented in Fig. 1 was prepared in the second campaign for which the MgF_2 film thicknesses were somewhat reduced to try to shift the low R_p region down to 121.6 nm; this sample is here called sample 2. The sample was measured ~2 months after deposition; the sample was in contact with normal air for about one week, and the rest of the time was stored in residual vacuum. The reflectance of this sample is presented in Fig. 2; the angle step was 2º and the spectral scanning was made in photon energy steps of 0.05 eV. The structure that is observable in Fig. 1 can be seen to have been correctly shifted to shorter wavelengths in Fig. 2, as expected. R_p at the wavelength of 121.6 nm and at the target angle (60º) was in the 0.01-0.02 range, but a value smaller than 0.01 was measured at the same wavelength and at angles in the 62º-68º range, with R_s in the range of 0.69 (62°) to 0.75 (68°). A value of R_p below 0.01 was measured at wavelengths between 119.8 nm (at 64º, R_s=0.68) and 129.1 nm (at 68º, R_s=0.76).

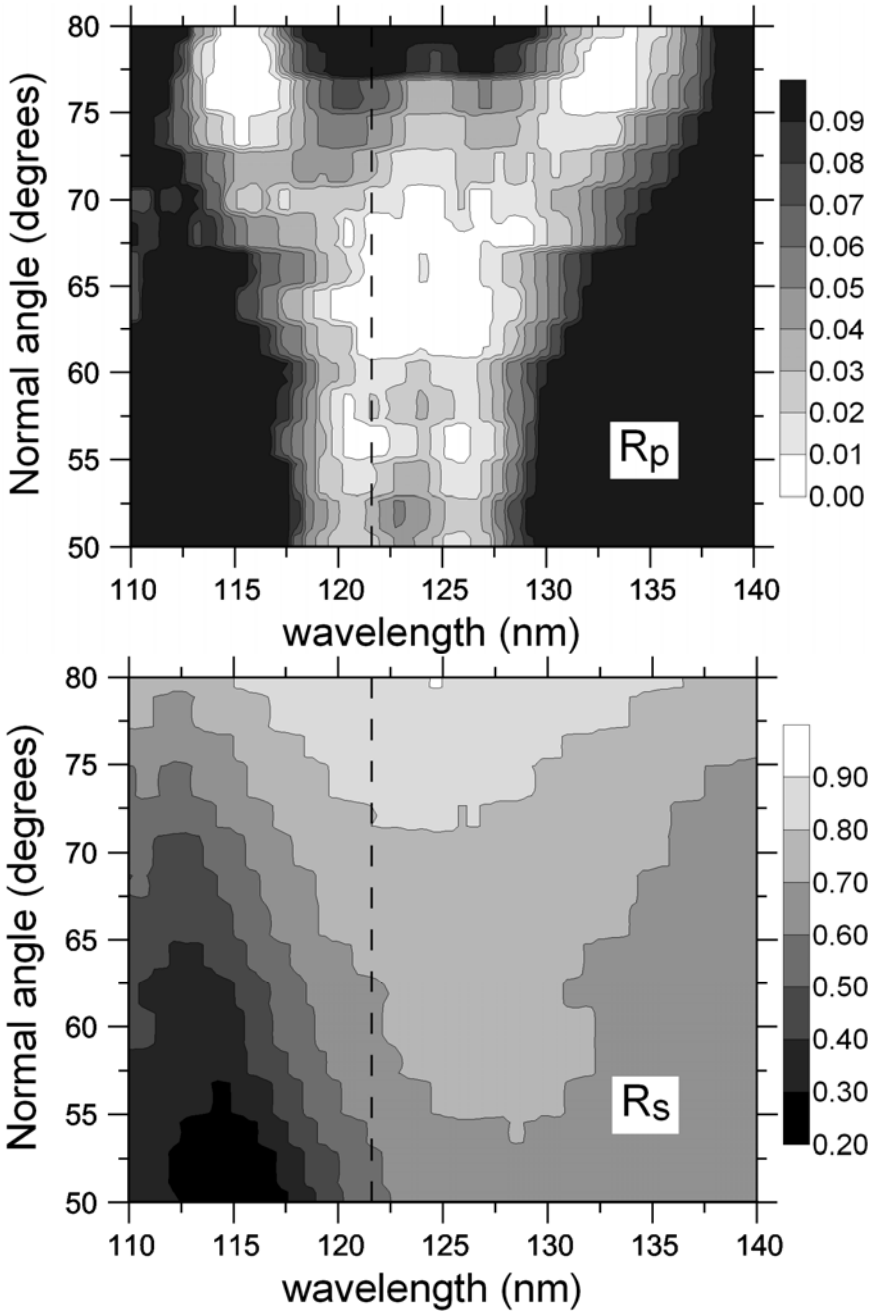

Fig. 2. Contour plots of R_p (top) and R_s (bottom) of sample 2 as a function of wavelength and normal incidence angle. The dashed line is at 121.6 nm

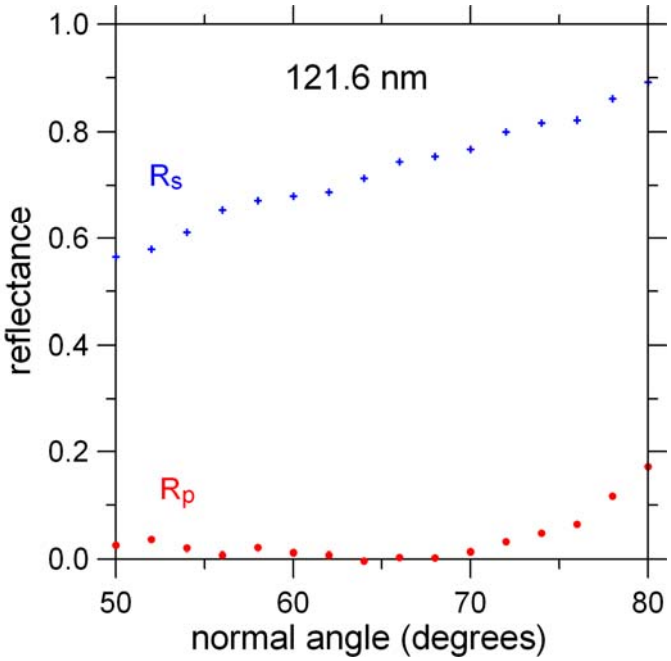

Fig. 3. R_p and R_s of sample 2 versus the normal incidence angle measured at 121.6 nm

Fig. 3 displays R_s and R_p versus incidence angle measured for sample 2 at 121.6 nm. The figure displays the wide angle range at which important linear polarization is produced. Comparing data in Fig. 3 with the data measured by Bridou et al.[17] for an $(Al/MgF_2)_2$ polarizer, the increase from two to three Al/MgF_2 bilayers results in a lower R_p in the whole angle range displayed and a larger R_s in the angle range above 56°, and similar below this angle. The $(Al/MgF_2)_2$ coating designed in Ref. 17 was reproduced by Kano et al.[18]; the latter resulted in R_p ~0.01 at 121.6 nm at 68º, lower than the original displayed in Ref. 17, and similar to the one measured here for sample 2; however, the coating of Ref. 18 displays a narrower angular band than the present one. Additionally, the coating of Ref. 18 displays a significantly lower R_s in the whole angle range. The present data also result in a larger R_s than all the one-layer or two-layer polarizers developed in Ref. 17.

Let us concentrate on the uncertainty in the measurement of small values on R_p. The aforementioned degree of linear polarization that is calculated for the vertical acceptance selected for the present measurements was 0.99, which means that the intensity ratio for the two perpendicular planes of incidence is ~200; this results in a theoretical contribution of 0.005 of the non-extinguished component when trying to measure the extinguished component, so that a virtual R_p=0 of an optimum coating would apparently increase to ~0.005xR_s. Furthermore, the weak signal that is available when R_p<~0.01 results in a source of uncertainty. The latter explains why a few measured data were slightly negative; as an example, in the low R_p range plotted in Fig. 2, 15 measurements were negative out of a total of 61 measurements below 0.01. When the signal is small, random variations of the background result in a significant uncertainty at low R_p, which can be either positive or negative. Since the present polarizing coatings provide a low value of R_p that is measured with a significant uncertainty in the current measurement conditions, two direction of improvement are envisaged. One is to reduce the vertical acceptance in order to increase the degree of polarization of the beam; unfortunately this results in still fewer photons. The other direction is to increase the detector integration time, even more if the beam is going to be weaker due to a smaller acceptance, and to do more measurement repetitions of the signal and the background to reduce statistical errors.

Fig. 4 displays R_p and R_s of sample 2 versus wavelength measured at 64º. At this angle, the spectral range with high R_s/R_p ratio is extended from 119.8 nm to 127.2 nm. As mentioned above, some spectral tuning is possible by changing the incidence angle.

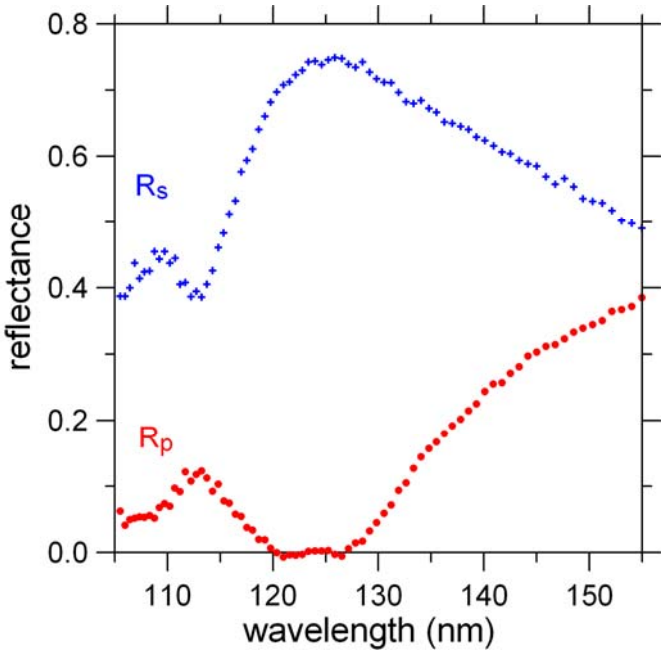

Fig. 4. R_p and R_s of sample 2 versus wavelength measured at 64º

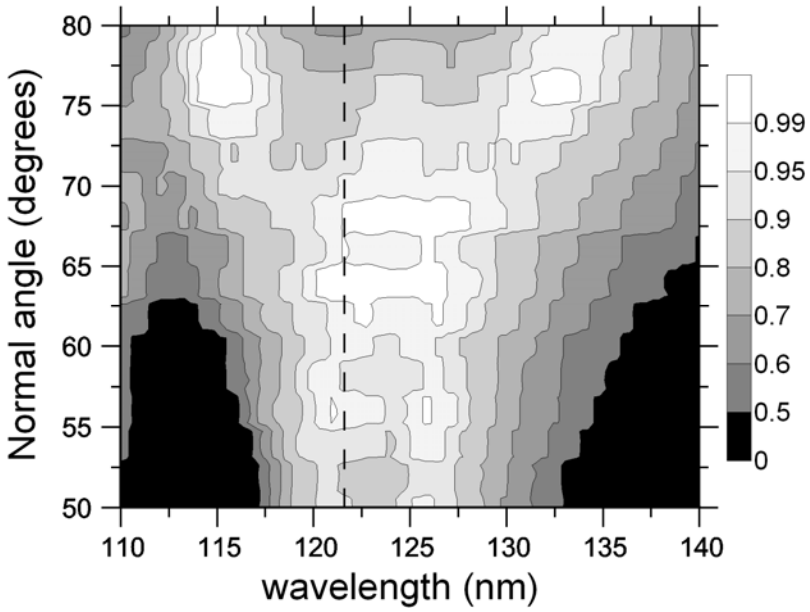

Fig. 5. Contour plots of polarizance measured for sample 2 as a function of wavelength and normal incidence angle. The dashed line is at 121.6 nm.

A parameter often used to evaluate the efficiency of a polarizer in providing linearly polarized light along a given direction of the electric field is the polarizance:

$$P = \frac{R_s - R_p}{R_s + R_p} \tag{1}$$

In the definition of P the opposite sign is often used; the present sign has been selected so that P is positive in the interesting cases. Other names have been used in the literature for the same magnitude represented by P, such as degree of polarization or polarizing power. We avoid using the term degree of polarization because it is also used in the literature with different meanings, and in fact it has been used above to state the proportion of linear polarization of the incoming beam. An optimum polarizer would have P=1. Fig. 5 plots P as a function of wavelength and the incidence angle. The more remarkable areas in Fig. 5 are those of P larger than 0.95 and 0.99.

Reflectance measurements were performed on samples that had been exposed to the atmosphere for about one week. At this time, no ageing studies have been performed on the polarizing coatings. Such studies are expected to be carried out in the near future.

CONCLUSIONS

Efficient polarizers based on $(Al/MgF_2)_3$ multilayer coatings have been designed, prepared, and their reflectance measured in two perpendicular planes of incidence for the purpose of developing a polarizer tuned at 121.6 nm. A first sample resulted in high R_s and R_s/R_p at the 127.5-130-nm spectral range. These results were used to refine the multilayer design in order to shift the spectral range of good polarization properties towards shorter wavelengths. A second sample so prepared resulted in excellent polarization properties with $R_p<0.01$ not only at 121.6 nm, but from ~119.8 nm (at 64º, $R_s=0.68$) to 129.1 nm (at 68º, $R_s=0.76$). A wide angle range of small R_p was measured at 121.6 nm. The measured performance is better than what had been reported in the literature so far. Measurements were performed on coatings that had been exposed to the atmosphere for about one week. New measurements on aged samples are expected in the near future.

ACKNOWLEDGMENTS

This work was supported by the National Programme for Research, Subdirección General de Proyectos de Investigación, Ministerio de Ciencia e Innovación, project number AYA2010-22032. L. Rodríguez-de Marcos is thankful to Consejo Superior de Investigaciones Científicas (Spain) for funding under the Programa I3P, partially supported by the European Social Fund. The technical assistance of J. M. Sánchez-Orejuela is acknowledged. We acknowledge the stimulus from J.-C. Vial and F. Auchère.

REFERENCES

[1] S. Sahal-Bréchot, "Role of collisions in the polarization degree of the forbidden emission lines of the Solar Corona. II - Depolarization by electron impact and calculation of the polarization degree of the Green line of Fe XIV", Astron. Astrophys. **36**, 355 (1974).
[2] V. Bommier, and S. Sahal-Bréchot, "The Hanle effect of the coronal Lα line of hydrogen: Theoretical investigation", Sol. Phys. **78**, 157-178 (1982).
[3] S. Fineschi, "Space-based Instrumentation for Magnetic Field Studies of Solar and Stellar Atmospheres", ASP Conf. Ser. **248**, 597-605 (2001).
[4] V. Bommier, "Hanle effect from a dipolar magnetic structure: the case of the solar corona and the case of a star", Astron. Astrophys. **539**, A122 (2012).
[5] S. Fineschi, R. B. Hoover, and A. B. C. Walker II, "Hydrogen Lyman α coronagraph/polarimeter", Proc. SPIE **1546**, 402-413 (1991).
[6] S. Fineschi, R. B. Hoover, M. Zukic, J. Kim, A. B. C. Walker II, and P. C. Baker, "Polarimetry of the HI Lyman α for coronal magnetic field diagnostics", Proc. SPIE **1742**, 423-438 (1992).
[7] S. Sahal-Bréchot, "The Hanle effect applied to magnetic field diagnostics", Space Sci. Rev. **29**, 391-401 (1981).
[8] S. Fineschi, R. B. Hoover, J. M. Fontenla, and A. B. C. Walker II, " Polarimetry of extreme ultraviolet lines in solar astronomy", Opt. Eng. **30**, 1161-1168 (1991).
[9] N.-E. Raouafi, P. Lemaire, and S. Sahal-Bréchot, "Detection of the O VI 103.2 nm line polarization by the SUMER spectrometer on the SOHO spacecraft", Astron. Astrophys. **345**, 999-1005 (1999).
[10] N.-E. Raouafi, , J. W. Harvey, and S. K. Solanki, "Properties of solar polar coronal plumes constrained by ultraviolet coronagraph spectrometer data", Astrophys. J. **658**, 643-656 (2007).
[11] W. C. Walker, "Pile-of-plates polarizer for the vacuum ultraviolet", Appl. Opt. **3**, 1457-1459 (1964).
[12] D. L. Steinrnetz, W. G. Phillips, M. Wirick, and F. F. Forbes, "A polarizer for the Vacuum Ultraviolet", Appl. Opt. **6**, 1001-1004 (1967).
[13] G. Hass and W. R. Hunter, "Reflection polarizers for the vacuum ultraviolet using Al + MgF_2 mirrors and an MgF_2 plate", Appl. Opt. **17**, 76-82 (1978).
[14] M. Yang, C. Cobet, and N. Esser, "Tunable thin film polarizer for the vacuum ultraviolet and soft x-ray spectral regions", J. Appl. Phys. **101**, 053114 (2007).
[15] J. Kim, M. Zukic, and D. G. Torr, "Multilayer thin film design as far ultraviolet polarizers", Proc. SPIE **1742**, 413-422 (1992).

[16] F. Bridou, M. Cuniot-Ponsard, J.-M. Desvignes, M. Richter, U. Kroth, and A. Gottwald, "Experimental determination of optical constants of MgF_2 and AlF_3 thin films in the vacuum ultra-violet wavelength region (60–124 nm), and its application to optical designs", Opt. Commun. **283**, 1351–1358 (2010).
[17] F. Bridou, M. Cuniot-Ponsard, J.-M. Desvignes, A. Gottwald, U. Kroth, and M. Richter, "Polarizing and non-polarizing mirrors for the hydrogen Lyman-α radiation at 121.6 nm", Appl Phys A **102**, 641–649 (2011).
[18] R. Kano, T. Bando, N. Narukage, R. Ishikawa, S. Tsuneta, Y. Katsukawa, M. Kubo, S.-N. Ishikawa, H. Hara, T. Shimizu, Y. Suematsu, K. Ichimoto, T. Sakao, M. Goto, Y. Kato, S. Imada, K. Kobayashi, T. Holloway, A. Winebarger, J. Cirtain, B. De Pontieu, R. Casini, J. Trujillo Bueno, J. Štěpán, R. Manso Sainz, L. Belluzzi, A. Asensio Ramos, F. Auchère, and M. Carlsson, "Chromospheric Lyman-alpha spectro-polarimeter (CLASP)", Proc. SPIE **8443**, 84434F (2012).
[19] S. Tolansky, "Multiple-beam interferometry of surfaces and films", Oxford University Press, London (1948).
[20] A. Giglia, N. Mahne, A. Bianco, C. Svetina, and S. Nannarone, "EUV soft X-ray characterization of a FEL multilayer optics damaged by multiple shot laser beam", Nucl. Instr. Meth. Phys. Res. A **635**, 530-538 (2011).
[21] G. Naletto, M. G. Pelizzo, G. Tondello, S. Nannarone, and A. Giglia, "The monochromator for the synchrotron radiation beamline X-MOSS at ELETTRA", Proc. SPIE **4145**, 105-113 (2001).
[22] S. Nannarone, A. Giglia, N. Mahne, A. De Luisa, B. P. Doyle, F. Borgatti, M. Pedio, L. Pasquali, G. Naletto, M. G. Pelizzo, and G. Tondello, "BEAR: a Bending Magnet for Emission Absorption and Reflectivity", Notiziario Neutroni e Luce di sincrotrone, **12**, 8-17 (2007).
[23] http://www.elettra.trieste.it/lightsources/elettra/elettra-beamlines/bear/beamline-description/page-7.html?showall=
[24] J. T. Cox, G. Hass, and J. E. Waylonis, "Further studies on LiF-overcoated aluminum mirrors with highest reflectance in the Vacuum Ultraviolet", Appl. Opt. **8**, 1535-1539 (1968).
[25] A. Daudé, M. Priol, and S. Robin, "Excitation par photons de plasmons de volume et de surface pour des couches de magnésium évaporées et étudiées en ultravide", C. R. Acad. Sci., Paris, **264**, 1489-1492 (1967).
[26] A. Daudé, A. Savary, G. Jezequel, and S. Robin, "Determination des constantes optiques du magnesium entre 500 et 1400 Å", Opt. Commun. **1**, 237-240 (1969).
[27] M. Vidal-Dasilva, A. L. Aquila, E. M. Gullikson, F. Salmassi, and J. I. Larruquert, "Optical constants of magnetron-sputtered magnesium films in the 25–1300 eV energy range", J. Appl. Phys. **108**, 063517 (2010).
[28] T. Ejima, A. Yamazaki, T. Banse, K. Saito, Y. Kondo, S. Ichimaru, and H. Takenaka, "Aging and thermal stability of Mg/SiC and Mg/Y_2O_3 reflection multilayers in the 25–35 nm region," Appl. Opt. **44**, 5446–5453 (2005).
[29] M. Fernández-Perea, R. Soufli, J. C. Robinson, L. Rodríguez-de Marcos, J. A. Méndez, J. I. Larruquert, and E. M. Gullikson, "Triple-wavelength, narrowband Mg/SiC multilayers with corrosion barriers and high peak reflectance in the 25-80 nm wavelength region", Opt. Exp. **20**, 24018-24029 (2012).
[30] G. Hass and R. Tousey, "Reflecting coatings for the Extreme Ultraviolet", J. Opt. Soc. Am. **49**, 593-602 (1959).
[31] E. Spiller, "High quality Fabry-Perot mirrors for the ultraviolet", Optik **39**, 118-125 (1973).
[32] B. Bates, and D. J. Bradley, "Interference filters for the far ultraviolet (1700 Å to 2400Å)", Appl. Opt. **5**, 971-975 (1966).
[33] E. T. Fairchild, "Interference filters for the VUV (1200-1900 Å)", Appl. Opt. **12**, 2240-2241 (1973).
[34] A. Malherbe, "Interference filters for the far ultraviolet", Appl. Opt. **13**, 1275-1276 (1974).
[35] M. Fernández-Perea, J. A. Méndez, J. A. Aznárez, and J. I. Larruquert, "Filters for World Space Observatory", in *The World Space Observatory Project-Spain*, A. I. Gómez de Castro, E. Verdugo, eds., Editorial Complutense, Madrid, 2006.